Global and Planetary Change 145 (2016) 30–41

Contents lists available at ScienceDirect

Global and Planetary Change

journal homepage: www.elsevier.com/locate/gloplacha

Large scale pantelleritic ash flow eruptions during the Late Miocene in central Kenya and evidence for significant environmental impact

L. Claessens [a,d,*], A. Veldkamp [b], J.M. Schoorl [a], J.R. Wijbrans [c], W. van Gorp [a], R. Macdonald [e,f]

[a] Soil Geography and Landscape group, Wageningen University, P.O. Box 47, 6700 AA Wageningen, The Netherlands
[b] Faculty ITC, University of Twente, P.O. Box 217, 7500 AE Enschede, The Netherlands
[c] Department of Earth Science, Vrije Universiteit, De Boelelaan 1085, 1081 HV Amsterdam, The Netherlands
[d] International Crops Research Institute for the Semi-Arid Tropics (ICRISAT), P.O. Box 39063, 00623 Nairobi, Kenya
[e] Environmental Science Division, Lancaster University, Lancaster LA1 4YQ, UK
[f] IGMiP Faculty of Geology, University of Warsaw, 02-089 Warszawa, Poland

ARTICLE INFO

Article history:
Received 7 July 2015
Received in revised form 15 June 2016
Accepted 17 August 2016
Available online 20 August 2016

Keywords:
Tuff
Ash flow
Ignimbrite
Vitrophyre
Peralkaline rhyolites
$^{40}Ar/^{39}Ar$ geochronology

ABSTRACT

In the area south-east of Mount Kenya, four previously unrecorded peralkaline rhyolitic (pantelleritic) ash flow tuffs have been located. These predominantly greyish welded and non-welded tuffs form up to 12 m thick units, which are sometimes characterized by a basal vitrophyre. The four flow units yielded $^{40}Ar/^{39}Ar$ ages ranging from 6.36 to 8.13 Ma, indicating a period of ~1.8 Ma of pantelleritic volcanic activity during the Late Miocene in central Kenya. Tentative compositional and age correlations with other known tuff deposits suggest that the pantelleritic tuffs originally covered 40,000 km^2 in central Kenya, extending much further than earlier recorded Pliocene tuffs. This newly identified magmatic phase occurred between the phonolitic flood eruptions (16–8 Ma) and the Pliocene tuff eruptions (6–4 Ma). The occurrence of multiple ash flow tuff deposits up to 150 km away from the inferred eruptive center(s) in the central sector of the Kenya Rift, indicates multi-cyclic peralkaline supereruptions during the Late Miocene. By analogy with more recent pantelleritic eruptions, the tuffs are thought to have been sulfur-rich; during eruption, they formed stratospheric aerosols, with significant environmental impact. The timing of the eruptions coincides with the shift towards more savannah-dominated environments in East Africa.

© 2016 Elsevier B.V. All rights reserved.

1. Introduction

The onset of uplift, rifting and associated volcanism in East Africa was recently constrained by the (re)discovery of a 17 Ma old whale fossil in the Turkana region in northern Kenya 740 km inland from the present-day coastline of the Indian Ocean at an elevation of 620 m (Wichura et al., 2015). Since its formation during the Miocene, the Kenya Rift Valley has been estimated to have erupted >150,000 km^3 of volcanic rocks (Smith, 1994). The majority of these eruptives belong to the Plateau phonolites phase that erupted between 16 and 8 Ma ago (Macdonald, 2003). In the central sector of the Kenya Rift this phase was followed by a more explosive phase depositing thick (100–300 m) sequences of welded and non-welded ash flows and air-fall tuffs, labeled 'Pliocene tuffs'(Smith, 1994; Fig. 1-A). A first broad correlation suggests that an area of 29,000 km^2 was covered by these deposits and that the ash flows were sourced in the Nakuru-Naivasha-Suswa area (McCall, 1967; Baker et al., 1988; Leat, 1991; Smith, 1994). The so-called 'Pliocene tuffs' cover a roughly circular area centered by Lake Naivasha and with a radius of approximately 90 km (Fig. 1). Various different tuff deposits are recognized with only a handful of reliable age determinations that range from 6.4 to 4.2 Ma (Jones and Lippard, 1979). The oldest dated tuffs are the Mau tuffs which consist of at least four ash flow units of peralkaline trachytic composition. The youngest two flows have K—Ar ages of 6.0–5.8 Ma (Jones and Lippard, 1979) indicating late Miocene emplacement. Despite these clear late Miocene ages, Smith (1994) assembled all mainly trachytic (alkalis-silica classification; Le Bas et al., 1992) tuff deposits and defined them as 'Pliocene tuffs', heavily relying on the correlation of all eastern tuffs, specifically the Kinangop tuff (5.7–3.4 Ma) in the Kinangop plateau (Baker et al., 1988). Other accurate $^{40}Ar/^{39}Ar$ age estimates of tuffs and related deposits were obtained at hominid sites such as the Tugen Hills (Kingston et al., 2002) and near Lake Turkana, where Late Miocene and Pliocene tuffs have been dated (Brown and McDougall, 2011). All these tuffs are considered to have originated in the central sector of the Kenyan Rift from several potential eruptive centers (Smith, 1994). During geological mapping of the area south and south-east of Mount Kenya, different tuff deposits were described (Bear, 1952; Fairburn, 1963, 1966). The tuffs are partly buried by predominantly phonolitic lava flows and volcanic debris avalanche deposits (agglomerates) of Mount Kenya, indicating an older origin. The main volcanic activity of Mount Kenya has recently been dated accurately and occurred between 5.27 and 2.8 Ma

* Corresponding author at: International Crops Research Institute for the Semi-Arid Tropics (ICRISAT), P.O. Box 39063, 00623 Nairobi, Kenya.
E-mail address: l.claessens@cgiar.org (L. Claessens).

http://dx.doi.org/10.1016/j.gloplacha.2016.08.006
0921-8181/© 2016 Elsevier B.V. All rights reserved.

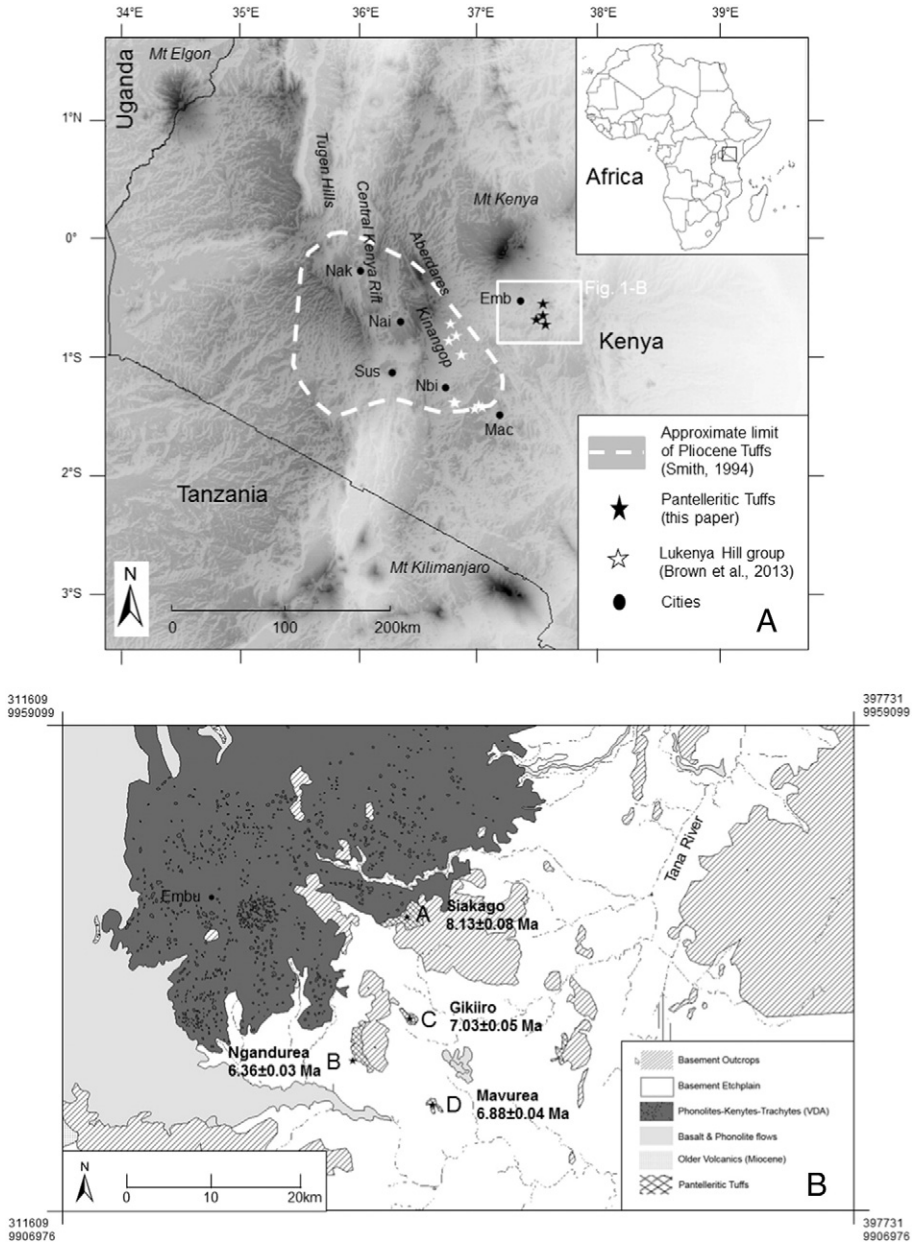

Fig. 1. Geological setting. (A) Location of study area and other localities within Kenya (Nak = Nakuru; Nai = Naivasha; Sus = Suswa; Nbi = Nairobi; Mac = Machakos; Emb = Embu). (B) Simplified regional geology map of the study area (after Bear, 1952) with the locations and ages of the tuffs. Note the depressions in the VDA deposit as mapped in Schoorl et al. (2014). Coordinates in UTM (zone 37).

($^{40}Ar/^{39}Ar$; Veldkamp et al., 2012; Schoorl et al., 2014). Somehow, these extensive tuff deposits have been ignored in Mio-Pliocene volcanic reconstructions. Given their location approximately 150 km east of the Kenya rift-axis, these tuffs can only have been deposited from large-scale, disruptive eruptions and may provide important information on distinct environmental changes and may be useful for palaeogeomorphological reconstructions of the region.

In order to resolve the origin and age of the tuffs south-east of Embu, exposures were mapped and sampled for geochemical analysis and $^{40}Ar/^{39}Ar$ dating. This paper aims to characterize the tuffs and to relate them to the Late Cenozoic geological and palaeoenvironmental history of central Kenya.

1.1. Study area

The study area is located in central Kenya and encompasses the eastern part of Embu County. Geological features in that setting include Mount Kenya volcanic deposits in the north and exposed Proterozoic metamorphic and crystalline rocks of the Mozambique Belt in the east and south (Bear, 1952; Fairburn, 1963; Veldkamp and Visser, 1992; Fig. 1-A). In the area south-east of Embu, volcanic tuffs have been found adjacent to, and below, Mount Kenya volcanic rocks (Bear, 1952; Fairburn, 1966; Fig. 1-A). These volcanic deposits have been correlated to the undated Nyeri tuffs and their origin has been preliminarily suggested in the Aberdares (Fairburn, 1966). More to the south, in the area north of Machakos and east of Thika, Fairburn (1963) mapped similar tuffs, which he referred to as the Athi tuffs. Later Baker et al., (1971, p. 199–200) correlated all these tuffs to the Plio-Pleistocene trachytic group.

Direct age estimates of the tuffs do not exist and only very tentative correlations have been explored. A palaeogeomorphological reconstruction of the Pliocene upper Tana basin raised questions about the age of the observed tuffs. It was suggested that some of the tuffs could have been related to main blocking phases of the

Tana River (Veldkamp et al., 2012). This would imply Pliocene ages (around 4 Ma) for the deposits. Based on this landscape reconstruction it is now also known that the volcanic debris avalanche (VDA) deposits of Mount Kenya overlying the tuffs south of Embu are around 2.8 Ma old (Schoorl et al., 2014).

Interestingly, the tuffs are found only above an elevation of 1100 m. All lower topographic features are integral parts of the erosional Tana valley, which started to incise at 2.8 Ma (Veldkamp et al., 2007). The Tana River has incised a 160 m deep valley, in which gravelly fluvial strath terraces with Quaternary ages have been recognized (Veldkamp et al., 2007). Due to the fluvial reorganizations of the upper Tana basin caused by a major volcanic debris avalanche event (around 2.8 Ma; Schoorl et al., 2014) and the emplacement of the Thiba flood basalt (0.8 Ma; Veldkamp et al., 2012), the Tana valley shifted southwards - and maintained the preservation of the tuff-containing area from further erosion.

2. Samples and methods

2.1. Fieldwork

Fieldwork consisted of an inventory, starting with previously mapped tuffs (Bear, 1952) and leading to the discovery of new deposits during different field campaigns (2008–2010, 2012, and 2014; Fig. 1-B). Table 1 gives a summary of the key locations discussed in this study. All encountered tuff units were sampled for $^{40}Ar/^{39}Ar$ dating and geochemical analysis. Samples were taken from fresh, non-weathered massive rock outcrops in building stone quarries. Local geomorphological mapping was based on a 30 m hole-filled seamless Shuttle Radar Topography Mission Digital Elevation Model (SRTM DEM; Reuter et al., 2007; Jarvis et al., 2008). In the field, hand-held GPS devices were used to register coordinates and altitudes of the sampling locations. The Universal Transverse Mercator (UTM) coordinates were linked to the SRTM

Table 1
Site locations and descriptions.

Site	Name location	UTM coordinates (UTM zone 37)	Description of lithology and structures
A	Siakago upper tuff	0349260–9938102	• Massive pale greyish homogeneous with weak columnar jointing (Fig. 3-A) • Fe and Mn staining on the rock surfaces • Numerous parallel oriented flattened whitish pumice fragments and an oriented vesicular structure • Locally imprints of reed • Total thickness is about 5 m • 0.8 m thick massive basal vitrophyre at the base • Resemblance to the Ngandurea upper tuff • 1–2 m thick red soil (Ferralsol) developed on top (Fig. 3-A)
	Siakago lower tuff	0349267–9938089	• Exposed as light grey massive columnar tuff outcrop at least 5 m thick • Homogenous and massive • No orientation in the pumice fragments • Minor small pumice and vegetation imprint fragments (reed and wood) • Frequently dark vesicular black and semi-rounded lithic fragments • Macroscopic sanidine feldspars but no basal obsidian glass • Dated sample location is 0349179–9938482 (1147 m) • Strongly resemblance to the Ngandurea lower tuff • Upper 2 m is weathered into dark reddish soil (Fig. 4-A) • Sometimes well-sorted greenish fluvial sand at the base
B	Ngandurea upper tuff	0343366–9922539	• Massive pale-grey homogeneous tuff with weak columnar jointing • Fe and Mn staining on the rock surfaces (Fig. 5) • Few inclusions of foreign material embedded in an irregularly greyish • Stained groundmass carrying numerous microlites • Clearly oriented compressed pumice fragments (Fig. 5-B) • Occasionally reed and wood imprints in an oriented vesicular structure (Fig. 6-B) • Resemblance to the Siakago upper tuff • 1–2 m thick red soil (Ferralsol) developed on top (see Fig. 5-A)
	Ngandurea upper tuff base	0343366–9922539	• 1 m thick basal vitrophyre characterized by clear orientation of compressed and flattened pumice fragments (both in greyish tuff as in vitrified base; see Fig. 5-B & C)
	Ngandurea lower tuff	0343463–9922529	• Total observed thickness is 6–8 m • Top is reddish due to weathering; lower in profile the color changes to a pale yellowish grey • Tuff is homogenous massive light grey • No orientation in the pumice fragments • Only a few small rounded pumice and vegetation imprint fragments (reed and wood) • Frequently dark vesicular black lithic fragments in the fragment are semi-rounded • High amount of sanidine feldspars but no obsidian glass • Tuff sequence is overlain by 1 m of solid obsidian (at 1188 m) • Strong resemblance to the Siakago lower tuff • Upper 3 m is weathered in reddish/pinkish grey colors (Fig. 7-A)
C	Gikiiro tuff	0349559–9927086	• Kari Phonolite overlying a 0.4 m thick sandy palaeosol (with hydromorphic features) in slope material developed on top of the tuff. • Tuff is massive greyish with no clear orientations and poor in lithic fragments • Coarse rounded pumice rich unit at the base • No obsidian glass • Maximum thickness is 5 m (Fig. 8)
D	Mavurea tuff top	0352002–9917711	• Sandy reddish soil (30 cm) followed by 70 cm “murram” (laterite) • Tuff is weathered along cracks and cemented by ironstone in root channels • Homogenous massive light grey • No orientation in the pumice fragments • Rarely small angular pumice and vegetation imprint fragments (reed and small wood) • Only a few rounded small fragments as inclusions (Fig. 9-B)
	Mavurea tuff base	0351842–9918084	• ~1 m massive black vitrophyre (see Fig. 9-C)

DEM. In this study the DEM altitudes were used to establish altitudes of locations.

2.2. $^{40}Ar/^{39}Ar$ dating

Samples were collected for $^{40}Ar/^{39}Ar$ dating from all four tuffs (see Figs. 1 and 2 for sample locations). Age estimates were obtained by incremental heating experiments carried out at the VU University, Amsterdam, the Netherlands (Schneider et al., 2009). Groundmass separates were prepared by obtaining homogenous fragments of microcrystalline groundmass to minimize the possibility of inherited argon from phenocryst phases (Wijbrans et al., 2011). For one sample (Ngandurea upper tuff) the sanidine phenocrysts were separated and dated separately. Data reduction and age calculations were made using ArArCalc v2.5 (Koppers, 2002). The detailed procedure is described in van Gorp et al. (2013), and Schoorl et al. (2014). Geochemical analyses were carried out at Activation Laboratories in Lancaster, Canada, using Fusion Inductively Coupled Plasma Emission (FUS-ICP). Subsequently, the methods can be found at http://www.actlabs.com/.

3. Results

3.1. Site descriptions

Four key sites were identified and studied in detail (Fig. 1; Table 1). Schematic cross-sections of the four sites are visualized in Fig. 2. In the original map by Bear (1952), seven patches of tuff deposits were large enough to be mapped. One of the map units was mistakenly attributed

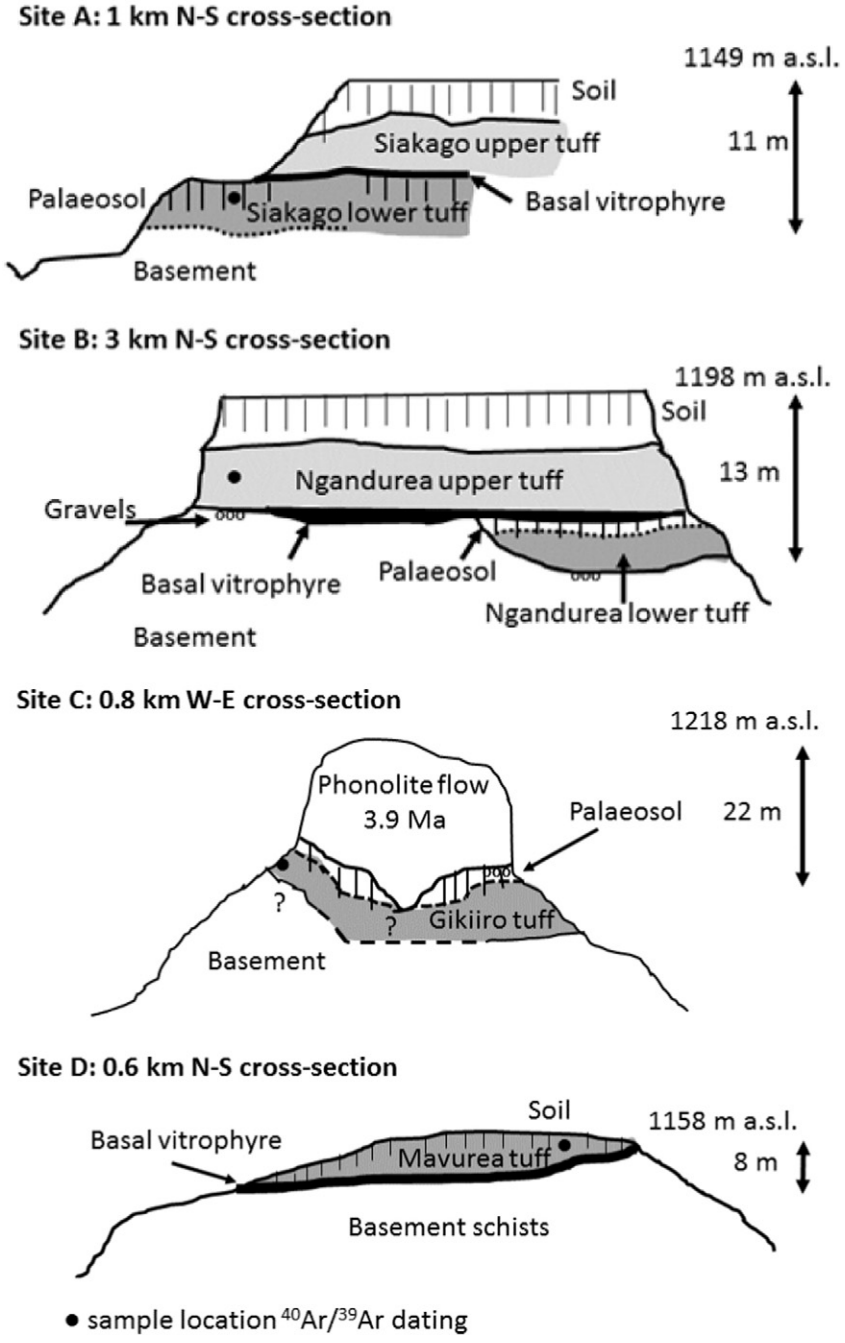

Fig. 2. Schematic cross-sections of the investigated four tuff sites: Siakago tuffs (site A), Ngandurea tuffs (site B), Gikiiro tuff (site C), and Mavurea tuff (site D). Abbreviations: a.s.l. (above sea level).

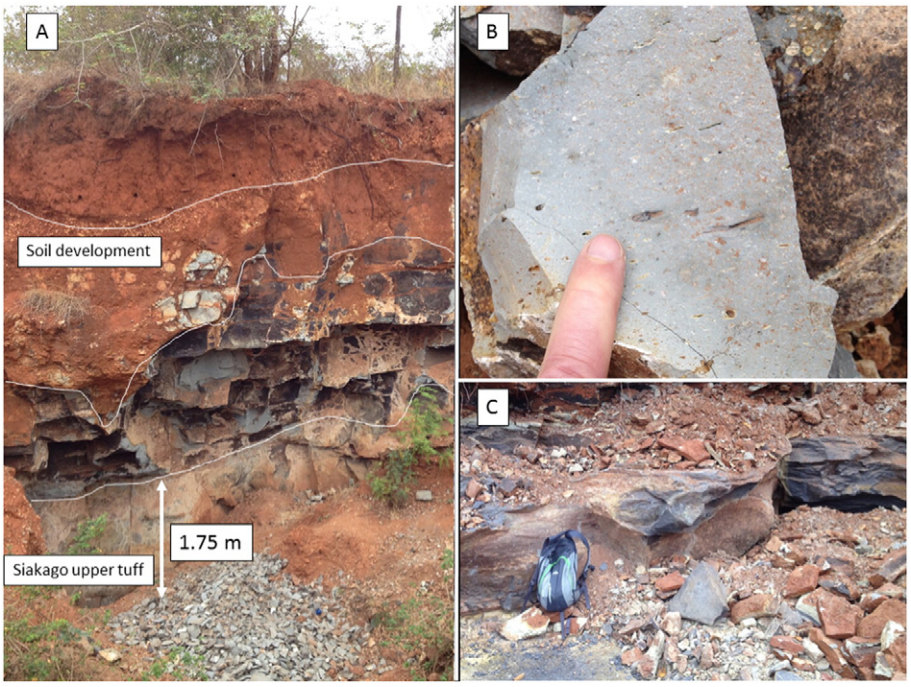

Fig. 3. Photographs of the Siakago upper tuff. (A) The General outcrop with thick soil development. (B) A close-up of the tuff. Note pale grey color and flattened pumice fragments. (C) The basal vitrophyre of the tuff.

to the here investigated tuffs. However, this unit is in fact a bottomland in the 2.8 Ma volcanic debris avalanche deposit (Schoorl et al., 2014). Originally Bear (1952) distinguished between two distinct tuff types: (a) a melanocratic gritty tuff north of Siakago (site A; Figs. 1-B and 2-A) and (b) a pale-grey homogeneous tuff at Ngandurea (site B; Figs. 1-B and 2-A). We revisited both key sites, and extended our study objects by two more tuff localities: (c) Gikiiro (site C; Figs. 1-B and 2-B) and (d) Mavurea (site D; Figs. 1-B and 2-B). The latter are building stone quarries, which provide sufficient outcrops and exposures to describe and sample the tuffs.

3.1.1. Site A: Siakago

An 11 m thick tuff crops out along the road (active and former building stone quarries) and in the river between an altitude of 1138 and 1149 m (Fig. 1-B). The tuffs comprise two units, the upper and lower tuffs, separated by a basal vitrophyre in the upper tuff. Both tuffs are grey massive, homogeneous and show weak columnar jointing (Fig. 2). The upper tuff (Fig. 3) is pale grey and demonstrates a clear orientation of flattened pumice fragments. The base of this unit consists of a vitrophyre up to 1 m thick (Fig. 3). Towards the north and east, the

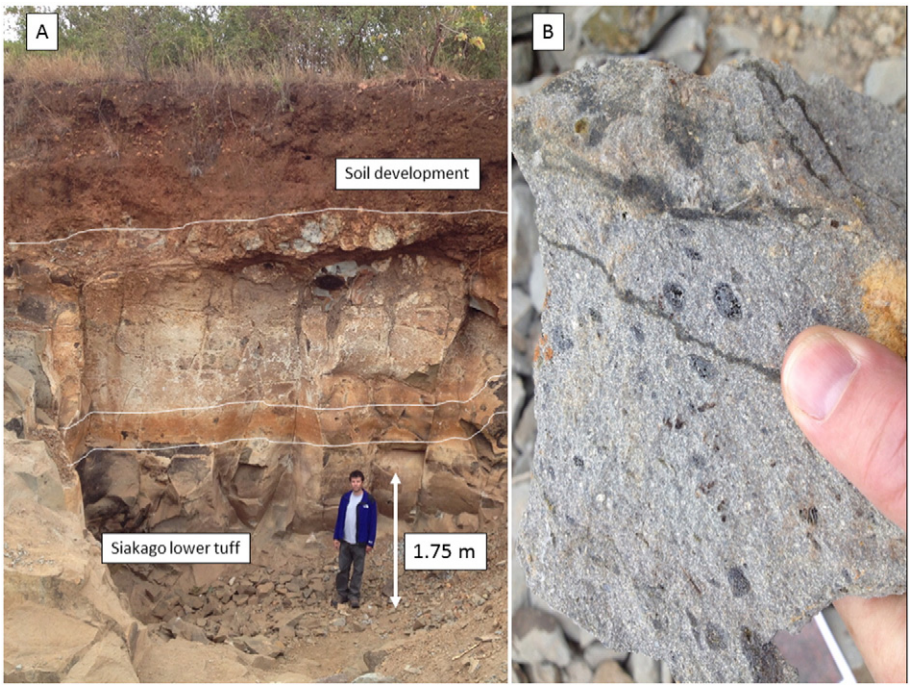

Fig. 4. Photographs of the Siakago lower tuff. (A) The general outcrop. Soil development is less due to truncation in slope position. (B) A close-up of the lower tuff with rounded dark vesicular fragments in a dark grey groundmass.

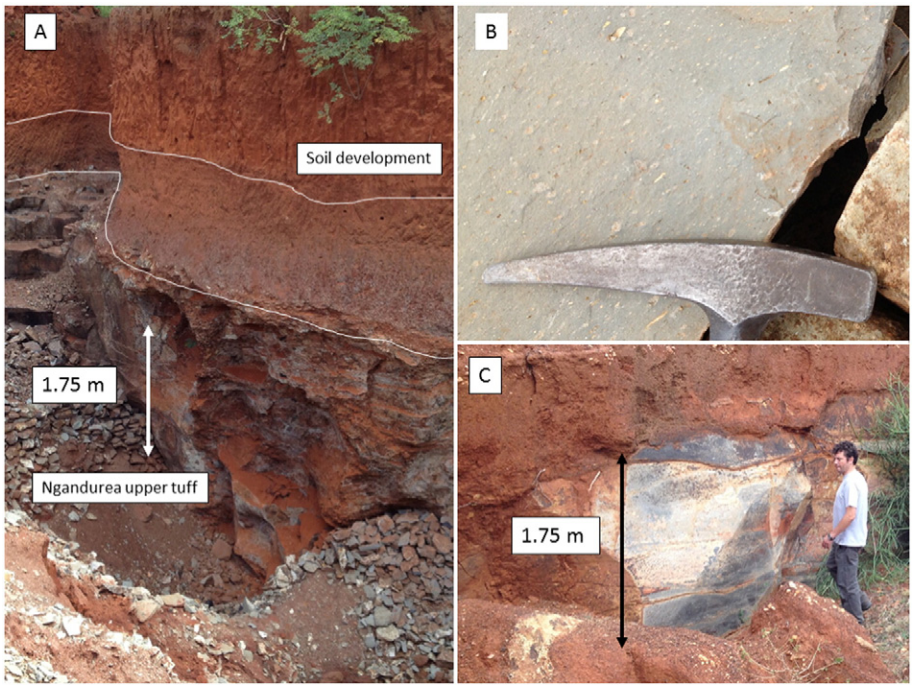

Fig. 5. Photographs of the Ngandurea upper tuff. (A) General outcrop with deep soil development. (B) A close-up of the tuff. Note pale grey color and flattened pumice fragments. (C) The thick basal vitrophyre of the tuff.

tuffs are buried by the 2.8 Ma Mount Kenya volcanic debris avalanche deposits (Schoorl et al., 2014). The lower tuff (Fig. 4) is dark grey and contains volcanic and non-volcanic lithic fragments, which are often rounded and follow the descriptions by Bear (1952) of the melanocratic gritty tuff. The base of the lower tuff is not clearly exposed, but no indications of glass were found near its base. A well-sorted greenish fluvial sand was observed at one location.

3.1.2. Site B: Ngandurea

Near the village of Ngandurea the tuffs form a long elongated, flat tilting terrace bench (6 × 2 km) between an altitude of 1221 and 1149 m. This prominent feature west of the granitic Kanjiro hill exhibits the largest visible tuff unit (Fig. 1). Along the edge many building stone quarries occur. Almost all the quarries mine the massive pale-grey homogeneous upper tuff (Figs. 2 and 5). The Ngandurea upper tuff forms a continuous, 5 to 7 m thick, unit that strongly resembles the Siakago upper tuff. The tuff has only a few lithic clasts embedded in a pale greyish groundmass carrying numerous microlites and displays clearly oriented flattened pumice fragments (Fig. 5). Twig and wood imprints are occasionally found (Fig. 6). Welding in these tuffs is commonly associated with streaks of obsidian or pumice fragments flattened parallel to the bedding. Towards the base of the tuff, more glass is observed and at

Fig. 6. More photographs of the Ngandurea upper tuff. (A) Vitric welded base of Ngandurea upper tuff, note the parallel orientation of the vesicals. (B) Fossil wood imprint in tuff.

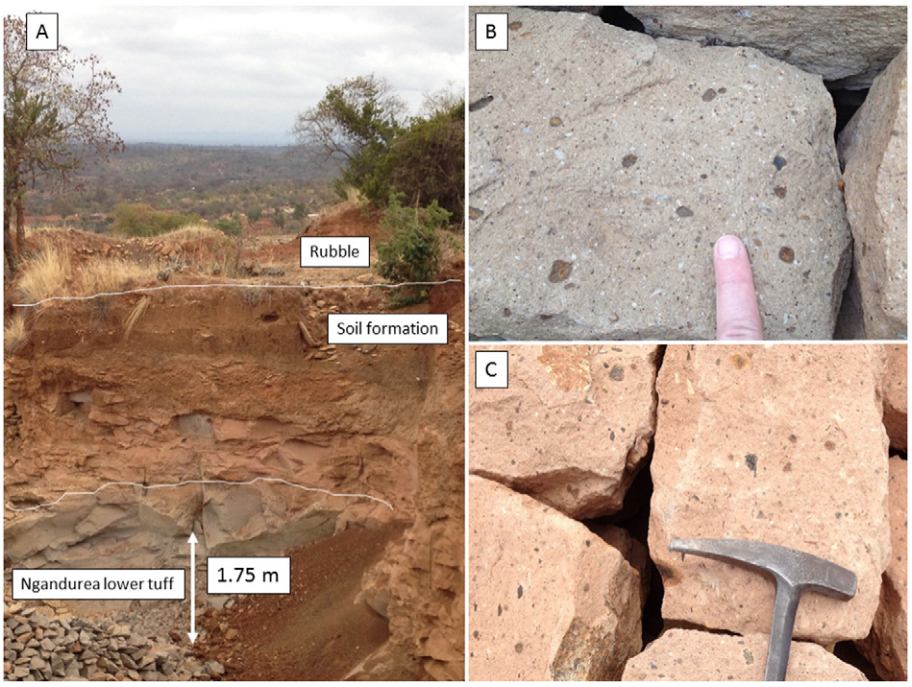

Fig. 7. Photographs of the Ngandurea lower tuff. (A) General outcrop. Soil development is less due to quarrying and slope position. Note the change in color from dark grey to more reddish colors from bottom to top. (B) A close-up of lower tuff with rounded dark vesicular fragments in a dark grey groundmass. (C) Same tuff but due to weathering a more reddish groundmass color.

some locations a 0.3 to 1 m thick massive vitrophyre forms the base of the Ngandurea upper tuff (Fig. 5). Fluvial gravels were found at a location where the Ngandurea tuff directly overlies basement system gneisses, indicating preservation in a former valley. Towards the south, the Ngandurea upper tuff (6 m) directly overlies granitic slope material and a reddish palaeosol formed in an underlying tuff (>6 m), which is grey lower down which strongly resembles the Siakago lower tuff (Figs. 4 and 7). This tuff has a reddish/pinkish greyish color at the top which becomes grey in the deeper parts of the unit (Fig. 7). The tuff does not display the same pumice orientation as the Ngandurea upper tuff (Fig. 5). It is rich in volcanic lithic fragments (dark basaltic to whitish pumice clasts), which are often rounded and less massive than in the overlying upper tuff. The base of this older tuff was not clearly exposed although no glass was observed near the base. Some gravels were found on the slope near the tuff-basement contact, again indicating deposition in a former valley. The total maximum accumulated thickness of the two tuff units is 13 m.

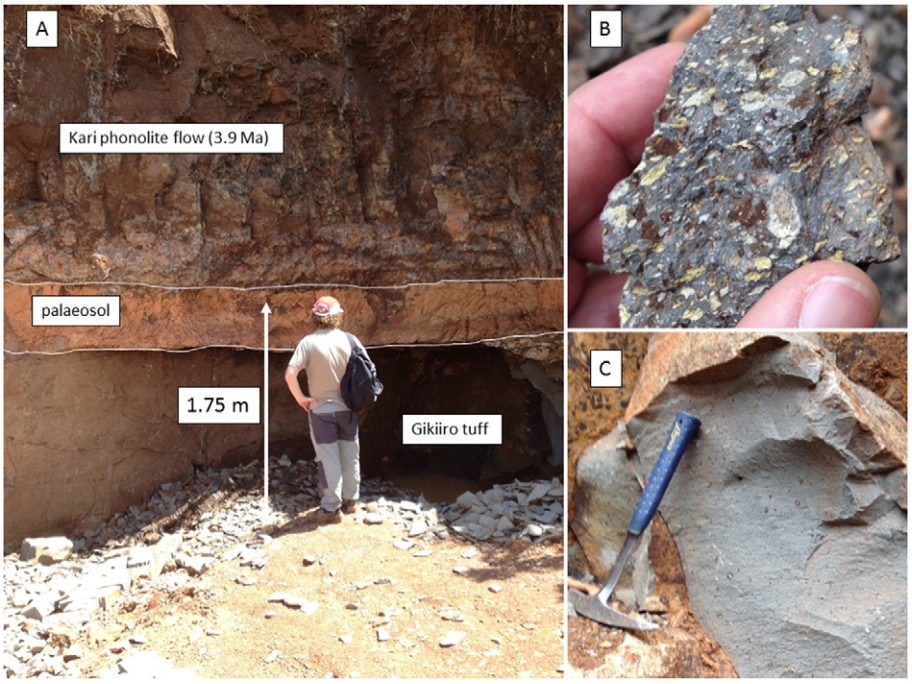

Fig. 8. Photographs of the Gikiiro tuff. (A) Overview of the Gikiiro tuff underlying Kari phonolite flow. The palaeosol in between has greyish hydromorphic features with murram (Fe_2O_3 iron-sesquioxide). (B) A close-up of the basal properties with many rounded pumice fragments. (C) A close-up of the greyish groundmass with no distinctive features.

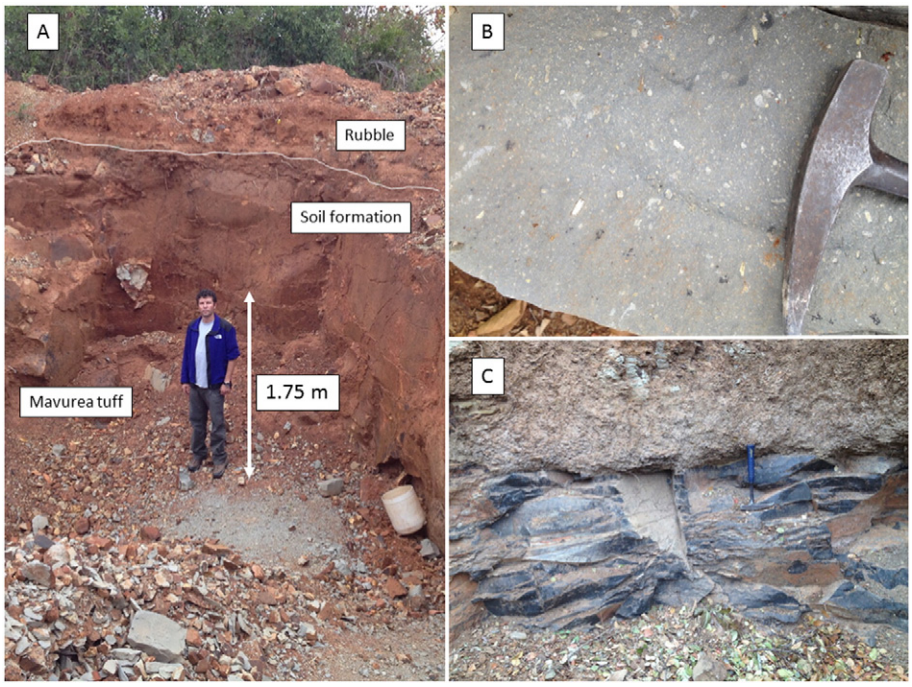

Fig. 9. Photographs of the Mavurea upper tuff. (A) An overview of the upper outcrops. (B) A close-up of the tuff with many small pumice and other inclusions. (C) The basal vitrophyre of the Mavurea tuff.

3.1.3. Site C: Gikiiro

Near Gikiiro the tuff crops out in various building stone quarries on the slope of a phonolite-capped hill at an altitude of 1218 m (Figs. 1-B and 2). These tuff outcrops occur all around the hill slope, indicating that the overlying 22 m thick dark Kari phonolite (3.9 Ma; Veldkamp et al., 2012) infills a shallow valley incised into the tuffs. Locally gravels are observed near the base of the phonolitic lava flow. Fig. 8 shows the Kari phonolite overlying a 0.4 m thick sandy palaeosol (with hydromorphic features) in slope material developed on top of the Gikiiro tuff. The Gikiiro tuff itself is a massive greyish tuff with no clear clast orientation and poor in lithic fragments. At the base a coarse, rounded pumice-rich unit occurs (Fig. 8). The maximum exposed thickness of the Gikiiro tuff is 5 m.

3.1.4. Site D: Mavurea

The Mavurea tuff (Figs. 1-B and 2) is exposed at only one locality where numerous small building stone quarries of maximum 5 m depth are found between an altitude of 1150 and 1158 m. The total thickness is about 8 m but no single outcrop exposes the entire unit. The base comprises a thick continuous and massive vitrophyre layer of approximately 1 m thickness (Fig. 9). The Mavurea tuffs have only a few irregular inclusions of foreign material (mainly wood and reed imprints and some un-orientated pumice fragments) embedded in a light greyish groundmass. The top of the unit is strongly cemented by ironstone and is overlain by sandy deposits containing murram (Fig. 9).

3.2. Geochemistry

Chemical analyses of the tuffs are presented in Table 2.

When the tuffs are classified using the alkalis-silica classification scheme, the Siakago lower tuff is considered as a dacite/trachyte, the Ngandurea upper tuff and the Gikiiro tuff as a trachyte, and the Mavurea tuff as a rhyolite. However, a problem in the analysis of pyroclastic rocks is that they are very prone to secondary hydration and consequent compositional modifications, especially the loss of Na and gain of Ca. The high loss of ignition values (up to 4.75 wt%), indicate that the studied tuffs have been hydrated, with significant loss of Na. Non-hydrated rocks of similar composition contain >6 wt% of Na_2O, as compared to the recorded values of <5 wt%. The loss of Na is important because it affects such features as the CIPW normative composition, the composition of the normative feldspar, and the rock classification on the total alkalis–silica plot (Le Bas et al., 1992).

The CIPW normative compositions (Table 2) demonstrate that none of the samples have normative corundum but they do have acmite with sodium metasilicate (ns), which is a measure of peralkalinity. Using the approach after Macdonald et al. (1987) for peralkaline silicic rocks, the tuffs have 24–30% normative quartz and are acmite-normative, indicating that they are peralkaline rhyolites. Following Macdonald's (1974) FeO_{tot}–Al_2O_3 diagram of peralkaline rhyolites, the tuffs are pantellerites, compositionally similar to the pantellerites from the type-locality, the island of Pantelleria, Italy (Fig. 10-A). In this diagram, the Siakago lower tuff is slightly more aluminous than the others, indicating derivation from a different magma. Differences between the tuffs are also seen in the trace element data; whilst some trace element ratios are about constant, e.g. Zr/Nb 5.3 (Fig. 10-B), others are more variable (e.g. Th/U 7–15; Zr/Y 13–26). The differences are compatible with the different ages of the tuffs, determined by comendites.

3.3. $^{40}Ar/^{39}Ar$ dating

All four ages are relatively accurately dated (Renne et al., 1998) and do not yield overlapping ages (Table 3). It clearly shows that the four identified units represent four different eruptions in time. The Siakago lower tuff and Ngandurea lower tuff are the oldest of the four. This is also confirmed by their topographic position. Both were strongly weathered for a prolonged period before they were buried by the 6.36 Ma upper tuffs. The deposition of the Gikiiro tuff is about 1.1 Ma younger, followed by the Mavurea tuff, the Siakago upper (not shown in the table) and the Ngandurea upper tuff, the youngest of the four with an age estimate of 6.36 Ma. For more information on the analytical procedure and dating consistency and reliability we refer to Appendix 1.

Table 2
Geochemical composition of the four tuffs (groundmass) FUS-ICP.

	Site A: Siakago lower tuff	Site B: Ngandurea upper tuff	Site C: Gikiiro tuff	Site D: Mavurea tuff
wt%				
SiO_2	66,55	68,32	66,88	69,36
TiO_2	0,54	0,56	0,56	0,47
Al_2O_3	10,01	9,42	9,57	8,64
FeO*	8,98	8,10	7,55	8,07
MnO	0,18	0,27	0,28	0,25
MgO	0,17	0,25	0,52	0,12
CaO	0,57	0,53	0,63	0,49
Na_2O	3,75	4,31	4,68	4,13
K_2O	3,56	4,22	4,09	4,33
P_2O_5	0,04	0,05	0,05	0,03
Total	94,35	96,03	94,81	95,89
ppm				
Ba	155	167	331	115
Sr	37	24	48	28
Rb	75	196	170	218
Y	71	110	85	88
Zr	1875	1433	1241	1623
Hf	42,1	34,1	29,5	37,7
Nb	355	270	235	302
Ta	21,8	18	15,1	19,4
Zn	360	410	430	430
Ga	46	42	41	41
Th	47,1	37,4	32,3	43,5
U	6,5	2,7	2,1	4,8
La	177	306	194	223
Ce	340	305	371	301
Pr	35,8	61,1	42,3	48,7
Nd	125	211	150	164
Sm	22,2	36,2	28,2	27,5
Eu	2,99	5,04	4,18	3,8
Gd	17,4	27,3	22,6	18,9
Tb	2,6	4,2	3,3	3,1
Dy	14,4	21,5	17,8	17,8
Ho	2,6	4	3,2	3,5
Er	2,6	4	3,2	3,5
Tm	1,08	1,57	1,29	1,7
Yb	6,9	10,1	8,3	11,4
Lu	1,12	1,68	1,38	1,86
CIPW norms (oxidation ratios after Middlemost, 1989)				
q	28,3	26,1	24,2	29,9
or	22,2	25,9	25,4	26,6
ab	33,4	25,9	27,8	21,1
ac	0,1	9	8,5	9
ns		0,4	1	1,2
di	2,4	2,1	2,6	2,1
hy	7,4	9,4	9,3	9,1
il	1,1	1,1	1,1	0,9
mt	5,1	–	–	–
ap	0,1	0,1	0,1	0,1

FeO* all Fe calculated as Fe^{2+}.

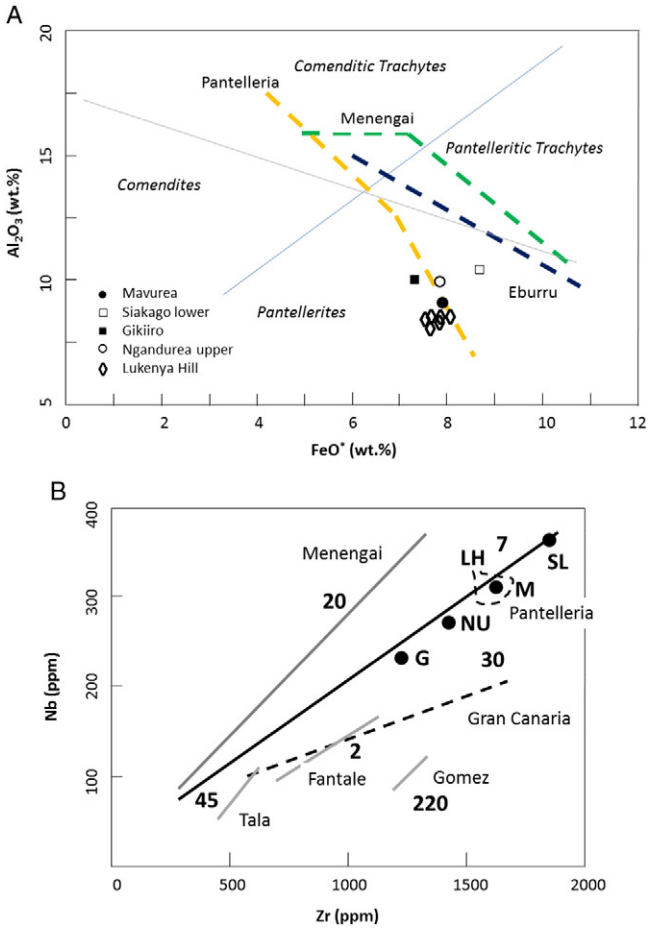

Fig. 10. Compositional comparison of tuffs from this study with others from the literature. (A) Classification scheme for peralkaline salic rocks of Macdonald (1974). The Miocene tuffs are pantellerites, closely similar to the type pantellerites from Pantelleria, Italy and to obsidians from the Lukenya Hill Group (Brown et al., 2013). Generalized compositional trends for Pantelleria and Eburru are from Macdonald et al. (2011). FeO* all Fe calculated as Fe^{2+}. (B) Zr—Nb plots of peralkaline ignimbrite units, showing the generalized compositional variation in the pre-eruptive magma chambers and the estimated volumes of each unit, in km^3. Also shown are data from this study (G, Giikiro; M, Mavurea; NU, Ngandurea upper; SL, Siakago lower; Table 2) and the Lukenya Hill tuff (LH, dashed field; Brown et al., 2013). Menengai, Kenya, first ash flow tuff; Green tuff, Pantelleria, Italy; Gran Canaria, ignimbrite A; Gomez tuff, Mexico; Fantale tuff, Ethiopia; Tala tuff, Mexico.
Modified from Macdonald (2012).

4. Discussion

4.1. Field observations

During field work it became clear from the macroscopic tuff characteristics that there are four tuff units. Near Siakago and Ngandurea, two tuffs with similar macroscopic properties overlie each other. There is no obvious relationship between these outcrops and the two localities near Gikiiro and Mavurea.

Based on observed field characteristics, all the tuffs have the properties of distal ash flow deposits. They have many oriented pumice and small rock fragments. They show various degrees of welding, from massive groundmass to basal vitrophyres. Taking the historic 1800 year old Taupo eruption in New Zealand as an analogue of a large-scale pyroclastic deposit (Walker et al., 1981), certain similarities may be observed. At Taupo, pyroclastic deposits are found in a roughly circular area at least 150 km from the central vent and pumice fragments have been observed up to 240 km from the eruptive center (Claessens et al., 2009). Within a 150 km radius of Taupo and up to 1 km above the eruption center, the landscape is covered by pyroclastic deposits. During their eruptions the pantelleritic pyroclastic flows in Kenya only had to overtop the rift valley shoulders. During the Late Miocene there was much less relief as the main rifting phase still had to occur (post Kinangop tuff phase, 3.4 Ma; Baker et al., 1988) and the Aberdares volcano complex (5–6.5 Ma; Baker et al., 1971, p. 205) did not exist yet. This implies that there were no large topographical barriers between the eruption center and the studied location during the Late Miocene.

Table 3
$^{40}Ar/^{39}Ar$ dating of the four tuffs.

Site and tuff	UTM coordinates (UTM zone 37)	$^{40}Ar/^{39}Ar$ age (Ma)
Site A: Siakago lower tuff	349179–9938482	8.13 ± 0.08
Site B: Ngandurea upper tuff	343608–9924886	6.36 ± 0.03
Site C: Gikiiro tuff	349525–9926913	7.03 ± 0.05
Site D: Mavurea tuff	352084–9917770	6.88 ± 0.04

Furthermore, in the Taupo area two types of deposits have been recognized: ignimbrite veneer deposits and valley pond deposits. The thicker ash rich valley pond (tuff) deposits form flat-floored bottom terraces in valleys up to 165 km from the collapsed caldera center. The Taupo tuff deposits at distances >50 km from the source have very fine textures, vitrophyres and no clear distinguishable banding or structures. These are all properties, which are also valid for our tuff deposits in Kenya. The flat-topped morphology, the underlying gravels, frequent fossil reed imprints or the fine textures, all imply that our tuff deposits are remnants of such pyroclastic valley pond deposits.

The fact that the oldest 8.13 Ma tuff is systematically covered by 6.36 Ma tuffs suggests that there was almost no uplift during the Late Miocene because both tuffs are valley pond deposits. If uplift had occurred between 8.13 and 6.36 Ma, the resulting fluvial incision would have caused the younger tuffs to be at lower topographic positions within an incised valley. As a reference, during the last 1 Ma the Tana river incised about 100 m (Veldkamp et al., 2007). This might also explain why there is no clear relationship between the different tuffs and altitude. Active uplift did occur from the Late Pliocene (Veldkamp et al., 2012) onwards, causing the Tana river to incise and driving erosion of the surrounding landscape. All landscape below 1100 m belongs to this younger incisional phase. As a result, relief inversion positioned the tuffs high up (>1100 m) in the current landscape so that the tuffs have preserved remnants of the Late Miocene topography. Combining all the field evidence suggests that we have found evidence of four different 'Taupo-like' eruptions during the Late Miocene in the central sector of the Kenyan Rift.

4.2. Geochemistry

All the analysed tuffs were formed from pantelleritic ash flows. Furthermore, they are highly evolved compositionally, suggesting a mature high-level magma reservoir (Mahood, 1984; Macdonald and Scaillet, 2006; Macdonald, 2012). True pantellerites are uncommon in the Kenyan Rift because Miocene pantellerite centers have been recorded only from northern Kenya (Watkins, 1987; McDougall and Watkins, 1988). However, these are too distant to be directly related to the study area tuffs. Perhaps the nearest compositional analogues in central Kenya come from the Eburru complex at Lake Naivasha (Ren et al., 2006; Fig. 1-A) but are too young to be directly related to the Late Miocene tuffs (<0.45 Ma; Clarke et al., 1990). Nevertheless, it is possible that the eruptive center(s) lay in the Naivasha region, in what Macdonald and Scaillet (2006) termed the central Kenya peralkaline province. The province comprises five young (<1 Ma) volcanic complexes dominated by peralkaline trachytes and rhyolites. It coincides with an area of crustal upwarping known as the Kenya dome, with its maximal topographic height near Lake Nakuru. The dome is apparently in isostatic equilibrium and is supported by the loading of anomalous mantle within the underlying lithosphere (Smith, 1994). It seems possible that this area of anomalous mantle generated the parental magmas (basalts?) and also promoted the Miocene peralkaline magmatism.

In a study of the chemical composition of Kenyan obsidians, Brown et al. (2013) identified one widespread, compositionally homogenous occurrence in an ash flow tuff, the so-called Lukenya Hill group (Fig. 1-A). This rhyolitic obsidian displays a uniform composition from Githumu (40 km south of Nyeri) to Lukenya (10 km west of Machakos) to the western Kenya rift-shoulders along the Mau-Escarpment (165 km to the west), overall covering an area of at least 8750 km^2. This area largely overlaps with the geographical projection of the four dated Miocene tuffs. In terms of major elements, it is also very similar to the tuffs, especially the Mavurea tuff (Table 2).

Furthermore, within the sedimentary sequence of the Miocene Tugen Hills (Fig. 1-A), a large trachytic ash flow deposit (Deino, pers. comm.), the so-called Mpesida Beds (Chapman and Brook, 1978; Kingston et al., 2002), has a similar $^{40}Ar/^{39}Ar$ age (6.36 Ma) to the Ngandurea tuffs. This might suggest a similar origin, but without geochemical compositional confirmation, no definite correlation can be established.

We have at least one group correlative tuff deposits (Lukenya Hill group) within Kenya, suggesting an even larger geographical spread than that delineated for the 'Pliocene tuffs' by Smith (1994). The 'Pliocene tuffs' were found around the central sector of the Kenyan Rift valley in an area with a radius of ~90 km (Fig. 1-A) it appears that the outcrops of the Late Miocene pantelleritic tuffs have a radius of 150 km (Fig. 1).

What is also striking is that the four tuffs fill a time gap in the magmatic history of central Kenya. In the most recent reconstruction (Macgregor, 2015) is a temporal gap in the volcanism between 8 Ma (end of the phonolitic flood eruptions) and the 5 Ma Kinangop tuffs. It appears that the large-scale, tuff-generating eruptions had already started in the Late Miocene, at around 8 Ma. These first eruptions were very far-reaching and generated pantellerites, indicating that the tuffs originated from shallow magma chambers after extensive magma fractionation histories during the Late Miocene.

4.3. Large scale eruptions

All four tuffs show characteristics of distal ash flow deposits, implying long travel distances. Furthermore, the inferred source area (central sector of the rift system) is 150 km to the west, pointing to four large-scale volcanic eruptions during the Late Miocene. Rhyolitic pyroclastic deposits are highly variable in bulk volume (0.1 to over 1000 km^3) and run-out distances (1 to over 100 km) (Freundt et al., 1999). The fact that pyroclastic flows can scale relief of up to 1000 m suggests that topography is not a major factor in determining the distance reached. Legros and Kelfoun (2000) demonstrated for the 186 AD Taupo eruption that a dilute current was responsible for transporting the ignimbrites to their limit. This system property appears to be also valid for our tuff-forming events. This implies that large-scale geometry ignimbrites such as the Miocene tuffs are dilute flow features from eruptions with high discharge rates (10^2–10^3 Mt/s).

Although varying in detail, the pantelleritic eruptions displayed in Fig. 10-B showed broadly similar histories. An initial tall plinian ash column can become gravitationally unstable and collapse (in part or in whole) to form an ash flow. During the initial phase, the ash particles and exsolved gas are capable to reach the stratosphere, where the gases are oxidized to SO_2 and form aerosols. Both, ash and aerosols, can be transported laterally for large distances but will eventually be deposited on the Earth's surface. Thus the deposits from peralkaline rhyolitic eruptions have been recorded at great distance from their source center. For example, ash from the relatively small Green Tuff eruption, Pantelleria (Fig. 10-B), has been recorded as far as the Dodecanese, some 1300 km east of Pantelleria (Margari et al., 2007).

4.4. Environmental impact of eruptions

Given that the Taupo eruptions in New Zealand had a significant environmental impact (Newnham et al., 1999), it is reasonable to infer an environmental signal related to the four large-scale Miocene eruptions. A recent reconstruction of Cenozoic vegetation in East Africa, based on a synthetic pollen diagram of the DSDP 231 marine core from the Gulf of Aden (Bonnefille, 2010), displays an aridity phase (see Fig. 9 in Bonnefille, 2010) between 6.3 and 8.0 Ma, the period during which the four reconstructed large-scale eruptions occurred (Fig. 11). Other studies based on pollen records from northern Kenya (Feakins et al., 2013) and carbon isotopes from herbivore teeth (Uno et al., 2011) show a distinct shift to drier conditions and widespread savannah vegetation during the same period. The most recent compilation of environmental and climate records relevant for Late Cenozoic African palaeoenvironmental change (Levin, 2015) gives the most comprehensive overview (Fig. 11). This figure contains relatively high resolution records of charcoal abundance (the fraction of charcoal relative to the

sum of pollen, charcoal, and spores) from ODP Site 1081 representing fire activity (Hoetzel et al., 2013) - and the proportion of *Poaceae* grass pollen (from ODP site 1081, 1082, 1085 and DSDP site 231; Bonnefille, 2010; Dupont et al., 2013; Feakins et al., 2013; Hoetzel et al., 2013). Within the range of given temporal uncertainties, the ages of our four tuff events correlate remarkably well with the charcoal and grass pollen records (Fig. 11). It appears that every major volcanic event coincides with a peak in charcoal abundance and they are often followed by an increase in grass pollen. This match may be coincidental but supports our suggestion that the large scale volcanic events may have helped to push the African vegetation stepwise towards more grass dominated vegetation types. Assuming the match is causal the charcoal peaks suggest that we might expect to find more large scale eruptions around 5.0, 5.8 and 6.4 Ma. As a matter of fact there are published Kenyan tuff ages known from 5.8 and 6.4 Ma (Jones and Lippard, 1979), but unfortunately we do not know the extent of these eruptions. It is only speculative, which mechanism caused the apparent correlation, but it suggests an African wide impact of the Late Miocene Kenyan eruptions. The volcanic eruptions seem to have contributed to both variability and instability, which caused not only regional but apparently also continental environmental change. Whether there is a causality between the vegetation change towards more grasslands and the large-scale eruptions remains to be investigated. All four tuffs have some fossilized wood fragments, pointing to the presence of trees in the environment during the ash flow eruption. However, these trees could have been local riparian valley vegetation as the tuffs are preserved only in pre-existing valleys. The eruptions certainly destroyed thousands of square kilometers of the existing ecosystems in central Kenya.

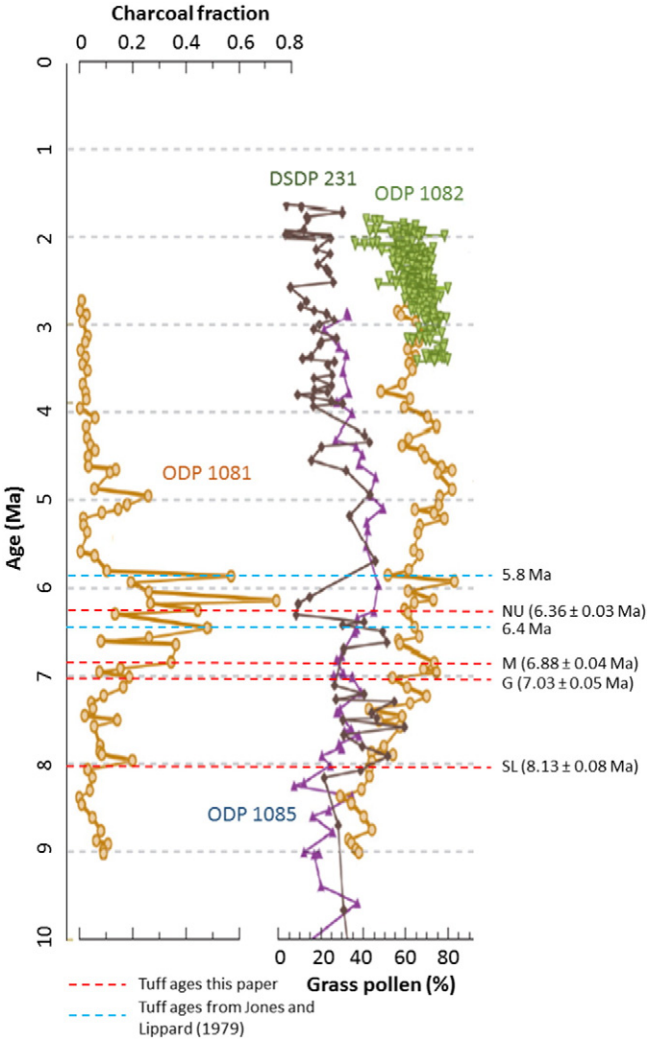

Fig. 11. A compilation of environmental and climate records relevant for Late Cenozoic African palaeoenvironmental change from Levin (2015). The source records are from the Atlantic Ocean off the western coast of Africa (ODP 1081, 1082, and 1085) and the Gulf of Aden (DSDP 231). These graphs display relatively high resolution records of charcoal abundance (the fraction of charcoal relative to the sum of pollen, charcoal, and spores) from ODP Site 1081 representing fire activity (Hoetzel et al., 2013), and the proportion of *Poaceae* grass pollen (from ODP site 1081, 1082, 1085; Bonnefille (2010), Dupont et al. (2013), Feakins et al. (2013), Hoetzel et al. (2013)). Red dashed lines are the dated tuffs of this study (G, Giikiro; M, Mavurea; NU, Ngandurea upper; SL, Siakago lower; Table 3). Blue dashed lines are other published Kenyan tuff ages (Jones and Lippard, 1979).

A contributory factor to the environmental effects of the peralkaline magmatism may have been the levels of sulfur emitted during the eruptions. Based on experiments and theoretical calculations, Scaillet and Macdonald (2006) showed that fluid/melt partition coefficients calculated for a pantellerite from Eburru are <50 at 1.5 kbar/800 °C and a bulk sulfur content of 1 wt%. Given their compositional similarities (Fig. 10-A and B), it is not unreasonable to assume that the Kenya tuffs had similar sulfur contents to the Pantellerian magmas. The high solubility of sulfur in peralkaline rhyolitic melts means that it is largely retained in the melt till eruption occurs. Using the Scaillet and Macdonald (2006) results as a basis, Neave et al. (2012) calculated that a relatively small pantelleritic eruption on Pantelleria, the 7 km^3 Green Tuff, had a sulfur yield of 80–160 Mt. Without knowledge of the sulfur content of the Miocene magmas, or estimates of the eruptive volumes, similar calculations of sulfur yield cannot be made. However, if the magmas had similar sulfur concentrations to Pantellerian pantellerites (up to 600 ppm; Neave et al., 2012), very significant amounts of sulfur were most likely injected into the atmosphere. Environmental consequences would have included surface temperature decrease, the direct effects of acid rain on the fauna and flora, and acidification of lakes. Recent simulations of similar scale eruptions and the effects of volcanic aerosols on climate forcing, indicate that grass covers recover much faster than forest, potentially leading to a competitive advantage of grass ecosystems (Timmreck et al., 2012). Therefore, we suggest that a series of these eruptions caused significant palaeoenvironmental changes and destroyed the regional vegetation of thousands of square kilometers in central Kenya. Probably grasses preferentially recolonized the extensive tuff-covered areas creating stepwise more extensive savannahs. This may have accelerated the transition of eastern African vegetation from forest towards more open savannah dominated environments, whereas at the same time in non-volcanic western Africa, a forest rich cover of the surface remained (Bonnefille, 2010).

Following the recent theories that lakes have been crucial in hominid evolution (Maslin et al., 2014), the related calderas (lakes) might have been instrumental in this evolution, too. The key component that Maslin et al. (2014) did not include in their theories of environmental control on early human evolution is volcanism. They made a convincing case about the role of climate and tectonics, but did not consider the direct and indirect effects of large volcanic eruptions in destroying and creating environments and lakes.

5. Conclusions

In the area south-east of Embu four ash flow tuffs have pantelleritic composition. The four units yield Late Miocene ($^{40}Ar/^{39}Ar$) ages ranging from 6.36 to 8.13 Ma. The tuffs seem to correlate well with one documented large scale tuff deposit (Lukenya Hill group). This is confirmed by the occurrence of large-scale pyroclastic deposits, which possibly originated from a precursor of the central Kenya peralkaline province in the Kenyan rift valley. Our observations imply that the peralkaline volcanic activity had already started in the Miocene. The fact that multiple thick tuff deposits have been preserved up to 150 km away from the inferred eruptive center(s) indicates multi-cyclic supereruptions during the Late Miocene. These eruptions destroyed existing

ecosystems, and created new environments, which may have been instrumental in contributing to the increase in savannah areal and human evolution during this period in East Africa.

Acknowledgements

Alan Deino is thanked for providing more background information about the Mpesida tuffs in the Tugen Hills. Fieldwork was partly supported by the CGIAR Research Program on Climate Change, Agriculture and Food Security (CCAFS). We thank Henry Wichura for useful suggestions and comments on an earlier version of the manuscript.

Appendix A. Supplementary data

Supplementary data to this article can be found online at http://dx.doi.org/10.1016/j.gloplacha.2016.08.006.

References

Baker, B.H., Williams, L.A.J., Miller, J.A., Fitch, F.J., 1971. Sequence and geochronology of the Kenya rift volcanics. Tectonophysics 11, 191–215.
Baker, B.H., Mitchell, J.G., Williams, L.A.J., 1988. Stratigraphy, geochronology and volcanotectonic evolution of the Kedong–Naivasha–Kinangop region, Gregory Rift Valley, Kenya. J. Geol. Soc. 145, 107–116.
Bear, L.M., 1952. A geological reconnaissance of the area south-east of Embu. Geol. Surv. Kenya Rep. 23.
Bonnefille, R., 2010. Cenozoic vegetation, climate changes and hominid evolution in tropical Africa. Glob. Planet. Chang. 72, 390–411.
Brown, F.H., McDougall, I., 2011. Geochronology of the Turkana depression of northern Kenya and southern Ethiopia. Evol. Anthropol. 20, 217–227.
Brown, F.H., Nash, B.P., Fernandez, D.P., Merrick, H.V., Thomas, R.J., 2013. Geochemical composition of source obsidians from Kenya. J. Archaeol. Sci. 40, 3233–3251.
Chapman, G.R., Brook, M., 1978. Chronostratigraphy of the Baringo Basin, Kenya. Geochem. Soc. Spec. Publ. 6, 207–223.
Claessens, L., Veldkamp, A., ten Broeke, E.M., Vloemans, H., 2009. A Quaternary uplift record for the Auckland region, North Island, New Zealand, based on marine and fluvial terraces. Glob. Planet. Chang. 68, 383–394.
Clarke, M.C.G., Woodhall, D.G., Allen, D., Darling, G., 1990. Geological, volcanological and hydrological controls on the occurrence of geothermal activity in the area surrounding Lake Naivasha, Kenya. British Geological Survey and Kenya Ministry of Energy. Derry and Sons Ltd, Nottingham (138 pp.).
Dupont, L., Rommerskirchen, F., Mollenhauer, G., Schefuss, E., 2013. Miocene to Pliocene changes in South African hydrology and vegetation in relation to the expansion of C4 plants. Earth Planet. Sci. Lett. 375, 408–417.
Fairburn, W.A., 1963. Geology of the North Machakos-Thika area. Geol. Surv. Kenya Rep. 59.
Fairburn, W.A., 1966. Geology of the Fort Hall area. Geol. Surv. Kenya Rep. 73.
Feakins, S.J., Levin, N.E., Liddy, H.M., Sieracki, A., Eglinton, T.I., Bonnefille, R., 2013. Northeast African vegetation change over 12 million years. Geology 41, 295–298.
Freundt, A., Wilson, C.J.N., Carey, S.N., 1999. Ignimbrites and block-and-ash flow deposits. In: Sigurdsson, H. (Ed.), Encyclopedia of Volcanoes. Academic Press, pp. 581–599.
Hoetzel, S., Dupont, L., Schefuss, E., Rommerskirchen, F., Wefer, G., 2013. The role of fire in Miocene to Pliocene C4 grassland and ecosystem evolution. Nat. Geosci. 6, 1027–1030.
Jarvis, A., Reuter, H.I., Nelson, A., Guevara, E., 2008. Hole-filled seamless SRTM data V4, International Centre for Tropical Agriculture (CIAT). available from http://srtm.csi.cgiar.org.
Jones, W.B., Lippard, S.J., 1979. New age determinations and the geology of the Kenya rift – Kavirondo Rift junction, West Kenya. J. Geol. Soc. Lond. 136, 693–704.
Kingston, J.D., Fine Jacobs, B., Hill, A., Deino, A., 2002. Stratigraphy, age and environments of the late Miocene Mpesida Beds, Tugen Hills, Kenya. J. Hum. Evol. 42, 95–116.
Koppers, A.A.P., 2002. ArArCALC- software for $^{40}Ar/^{39}Ar$ age calculations. Comput. Geosci. 28, 605–619.
Le Bas, M.J., Le Maitre, L.W., Woolley, A.R., 1992. The construction of the Total Alkali-Silica chemical classification of volcanic rocks. Mineral. Petrol. 46, 1–22.
Leat, P.T., 1991. Volcanological development of the Nakuru area of the Kenya rift valley. J. Afr. Earth Sci. 13, 483–498.
Legros, F., Kelfoun, K., 2000. On the ability of pyroclastic flows to scale topographical obstacles. J. Volcanol. Geotherm. Res. 98, 235–241.
Levin, N.E., 2015. Environment and climate of early human evolution. Annu. Rev. Earth Planet. Sci. 432, 405–429.
Macdonald, R., 1974. Nomenclature and petrochemistry of the peralkaline oversaturated extrusive rocks. Bull. Volcanol. 38, 498–516.
Macdonald, R., 2003. Magmatism of the Kenya Rift Valley: a review. Transactions of the Royal Society of Edinburgh: Earth Sciences 93, 239-253. J. Petrology 28, 979–1008.
Macdonald, R., 2012. Evolution of peralkaline silicic complexes: lessons from the extrusive rocks. Lithos 152, 11–22.
Macdonald, R., Scaillet, B., 2006. The central Kenya peralkaline province: insights into the evolution of peralkaline salic magmas. Lithos 91, 59–73.
Macdonald, R., Davies, G.R., Bliss, C.M., Leat, P.T., Bailey, D.K., Smith, R.L., 1987. Geochemistry of High-silica Peralkaline Rhyolites, Naivasha, Kenya Rift Valley.
Macdonald, R., Bagiński, B., Leat, P.T., White, J.C., Dzierżanowski, P., 2011. Mineral stability in peralkaline silicic rocks: insights from trachytes of the Menengai volcano, Kenya Rift Valley. Lithos 125, 553–568.
Macgregor, D., 2015. History of the development of the East African Rift System: a series of interpreted maps through time. J. Afr. Earth Sci. 101, 232–252.
Mahood, G.A., 1984. Pyroclastic rocks and calderas associated with strongly peralkaline magmatism. J. Geophys. Res. 89, 8540–8552.
Margari, V., Pyle, D.M., Bryant, C., Gibbard, P.L., 2007. Mediterranean tephra stratigraphy revisited: results from a long terrestrial sequence on Lesvos Island, Greece. J. Volcanol. Geotherm. Res. 163, 34–54.
Maslin, M.A., Brierley, C.M., Milner, A.M., Shultz, S., Trauth, M.H., Wilson, K.E., 2014. East African climate pulses and early human evolution. Quat. Sci. Rev. 101, 1–17.
McCall, G.J.H., 1967. Geology of the Nakuru-Thomson's Falls-Lake Hannington area. Geol. Surv. Kenya Rep. 78.
McDougall, I., Watkins, R.T., 1988. Potassium–argon ages of volcanic rocks from northeast of Lake Turkana, northern Kenya. Geol. Mag. 125, 15–23.
Middlemost, E.A.K., 1989. Iron oxidation ratios, norms and the classification of volcanic rocks. Chem. Geol. 77, 19–26.
Neave, D.A., Fabbro, G., Herd, R.A., Petrone, C.M., Edmonds, M., 2012. Melting, differentiation and degassing at the Pantelleria volcano, Italy. J. Petrol. 53, 637–663.
Newnham, R.M., Lowe, D.J., Williams, P.W., 1999. Quaternary environmental change in New Zealand: a review. Prog. Phys. Geogr. 23, 567–610.
Ren, M., Anthony, E.Y., Omenda, P.A., White, J.C., Macdonald, R., Bailey, D.K., 2006. Application of the QUILF thermobarometer to the peralkaline trachytes and pantellerites of the Eburru volcanic complex, East African Rift, Kenya. Lithos 91, 109–124.
Renne, P.R., Karner, D.B., Ludwig, K.R., 1998. Radioisotope dating - absolute ages aren't exactly. Science 282 (5395), 1840–1841.
Reuter, H.I., Nelson, A., Jarvis, A., 2007. An evaluation of void filling interpolation methods for SRTM data. Int. J. Geogr. Inf. Sci. 21, 983–1008.
Scaillet, B., Macdonald, R., 2006. Experimental and thermodynamic constraints on the sulphur yield of peralkaline and metaluminous silicic flood eruptions. J. Petrol. 47, 1413–1437.
Schneider, B., Kuiper, K., Postma, O., Wijbrans, J., 2009. $^{40}Ar/^{39}Ar$ geochronology using a quadrupole mass spectrometer. Quat. Geochronol. 4, 508–516.
Schoorl, J.M., Veldkamp, A., Claessens, L., van Gorp, W., Wijbrans, J.R., 2014. Edifice growth and collapse of the Pliocene Mt. Kenya: evidence of large scale debris avalanches on a high altitude glaciated volcano. Glob. Planet. Chang. 123, 44–54.
Smith, M., 1994. Stratigraphic and structural constraints on mechanism of active rifting in the Gregory rift, Kenya. Tectonophysics 236, 3–22.
Timmreck, C., Graf, H.-F., Zanchettin, D., Hagemann, S., Kleinen, T., Krüger, K., 2012. Climate response to the Toba super-eruption: regional changes. Quat. Int. 258, 30–44.
Uno, K.T., Cerling, T.E., Harris, J.M., Kunimatsu, Y., Leakey, M.G., Nakatsukasa, M., Nakaya, H., 2011. Late Miocene to Pliocene carbon isotope record of differential diet change among East African herbivores. Proc. Natl. Acad. Sci. 108, 6509–6514.
van Gorp, W., Veldkamp, A., Temme, A.J.A.M., Maddy, D., Demir, T., van der Schriek, T., Reimann, T., Wallinga, J., Wijbrans, J., Schoorl, J.M., 2013. Fluvial response to Holocene volcanic damming and breaching in the Gediz and Geren rivers, western Turkey. Geomorphology 201, 430–448.
Veldkamp, A., Visser, P.W., 1992. Erosion surfaces in the Chuka-South area, central Kenya. Z. Geomorphol. Suppl. 84, 147–158.
Veldkamp, A., Buis, E., Wijbrans, J.R., Olago, D.O., Boshoven, E.H., Marée, M., van den Berg van Saparoea, R.M., 2007. Late Cenozoic fluvial dynamics of the River Tana, Kenya, an uplift dominated record. Quat. Sci. Rev. 26, 2897–2912.
Veldkamp, A., Schoorl, J.M., Wijbrans, J.R., Claessens, L., 2012. Mount Kenya volcanic activity and the Late Cenozoic landscape reorganisation in the upper Tana fluvial system. Geomorphology 145–146, 19–31.
Walker, G.P.L., Wilson, C.J.N., Froggatt, P.C., 1981. An ignimbrite veneer deposit: the trail-marker of a pyroclastic flow. J. Volcanol. Geotherm. Res. 9, 409–421.
Watkins, J.L., 1987. Geology of Kubi Algi and Derati mountains, pantellerite bodies of Miocene age from the northern part of the Kenyan Rift Valley. J. Afr. Earth Sci. 6, 603–616.
Wichura, H., Jacobs, L.L., Lin, A., Polcyn, M.J., Manthi, F.K., Winkler, D.A., Strecker, M.R., Clemens, M., 2015. A 17-My-old whale constrains onset of uplift and climate change in east Africa. Proc. Natl. Acad. Sci. 112, 3910–3915.
Wijbrans, J., Schneider, B., Kuiper, K., Calvari, S., Branca, S., De Beni, E., Norini, G., Corsaro, R.A., Miraglia, L., 2011. $^{40}Ar/^{39}Ar$ geochronology of Holocene basalts; examples from Stromboli, Italy. Quat. Geochronol. 6, 223–232.